Hindawi
Wireless Communications and Mobile Computing
Volume 2022, Article ID 1455526, 11 pages
https://doi.org/10.1155/2022/1455526

Research Article

Adaptive Channel Estimation for Underwater Acoustic OFDM System in Impulsive Noise Environment

Yaohui Wu,[1] Pengfei Shao ,[1] Shaozhong Zhang ,[1] and Youming Li[2]

[1]*School of Information and Intelligent Engineering, Zhejiang Wanli University, Ningbo 315100, China*
[2]*Faculty of Electrical Engineering and Computer Science, Ningbo University, Ningbo 315211, China*

Correspondence should be addressed to Pengfei Shao; cbb_bb@126.com

Received 20 October 2021; Revised 9 December 2021; Accepted 18 December 2021; Published 17 January 2022

Academic Editor: Jian Su

Applying the orthogonal matching pursuit (OMP) to estimate the underwater acoustic (UWA) orthogonal frequency division multiplexing (OFDM) channels is attractive because of its high estimation accuracy and low computational cost. However, most existing OMP-based algorithms suffer the limited estimation accuracy in impulsive noise (IN) cases. Through the studies can be found, only part of channels' estimation is affected due to the random IN which appears transient and intermittent in time and frequency. Based on this observation, joint time-frequency OMP (JTF-OMP) method is proposed, where the estimation of the affected channels benefits adaptively from that of adjacent channels in time or frequency. It is well known that preliminary Doppler scale estimation is key to the subsequent OMP algorithm, which is difficult to deal with due to the IN. To solve this problem, an adaptive Doppler scale estimation (ADSE) method is proposed. It involves generating two shorter identical cyclic prefixes (CPs) for each OFDM symbol, placed before two adjacent OFDM symbols. The repetition pattern can adaptively defend the IN which appears randomly and shortly in time. Simulation results show that the proposed algorithms integrating JTF-OMP with ADSE can achieve much higher estimation accuracy and better system reliability than the OMP in the IN environment.

1. Introduction

The increasing marine service requirements urgently need to enhance the data rate of underwater acoustic (UWA) communication [1, 2]. However, the UWA channels at the physical layer are facing many challenges for high speed communication, such as long delay spread, significant Doppler scale, and severe channel attenuation [3]. Orthogonal frequency division multiplexing (OFDM) is recognized as an effective technique to meet the challenges, due to its robustness against frequency selectivity and interference [4]. To improve UWA OFDM system, instantaneous channel state information (CSI) through channel estimation is required, which is the basis of adaptive resource allocation at the transmitter and stable signal detection at the receiver [5].

By modeling and estimating the UWA channels as a basis expansion model (BEM), the time-varying nature of the channels can be modeled arbitrarily well [6, 7]. However, the BEM method alone will become more inefficient with much longer delay spread or larger Doppler scale of the UWA channels. The effective way to solve this problem is to exploit the fact that UWA channels are naturally sparse, i.e., most channel energy is concentrated in a few delay and/or Doppler values [8]. In recent years, to make full use of the sparsity of the UWA channels, compressed sensing (CS) algorithms have been applied to the UWA channel estimation, such as basis pursuit (BP), matching pursuit (MP), and orthogonal matching pursuit (OMP) [9, 10]. Among them, OMP algorithm is the most representative one, which can achieve high estimation accuracy with low computational complexity [11]. To fully exploit its potential in the UWA channel estimation, lots of related research is in progress. By adaptive iteration and gradient descent with sparse signal, an adaptive gradient descent OMP algorithm is proposed in [12], where the process of signal reconstruction is transformed to the unconstrained optimization problem. A look-ahead backtracking OMP-based sparse channel estimation technique is developed in [13], where the Doppler scale

is estimated and compensated by PN sequence in time domain. A novel and computationally efficient channel estimation algorithm is proposed in [14]; the OMP algorithm is combined with the maximum a posteriori probability (MAP) technique to estimate the UWA channel gains. A greedy algorithm technique of the OMP implemented with the BEM is proposed in [15], where no prior information about channel statistics is required and the spectral leakage can be avoided. To make the expansion coefficients uncorrelated with the increasement of the OFDM frame length, time-varying complex-valued channel path gains are estimated using BEM based on the orthonormal discrete Legendre polynomials [16]. To determine an appropriate iteration termination condition, [17] derives an adaptive OMP (A-OMP) algorithm based on the power ratio of the residual vector, where the recovery sparsity of the UWA channels is exploited.

Most of the aforementioned works assume that impulsive noise (IN) can be ignored in the UWA system; hence, they suffer the limited estimation accuracy in the IN cases. Unfortunately, due to human activities as well as natural sources, IN is frequently encountered, and it cannot be completely removed at the receiver by using blanking or clipping techniques [18]. Accordingly, joint channel and IN estimation methods have attract attention. The proposed method in [19] adopts the generalized approximate message passing (GAMP) to jointly estimate the channel and the IN, which assumes that a priori statistics about the IN can be acquired. Two pilot-subcarrier-based joint algorithms are proposed in [20] to improve the performance of channel estimation and IN mitigation, but the accurate positions of the IN are required in the received OFDM signal. A recursive CS algorithm incorporating Kalman filter and Smoother (KFS) is developed in [21], which adopts the sparse Bayesian learning (SBL) to construct the CS framework. However, these methods either require extra bandwidth for null subcarriers or use the statistical feature of the IN as the basis for instantaneous estimation.

In fact, the IN in the UWA system is very complex and difficult to be classified into a specific statistical characteristic. Furthermore, the statistical value of the IN may be quite different from the instantaneous value. Through the studies can be found, only part of the UWA channels' estimation is affected due to the random IN which appears transient and intermittent in time and frequency. According to literature [17], the IN will lead to huge channel gain variations on the elements of the estimated channels, and the iteration should be terminated early in the process of the OMP algorithm. In view of these, joint time-frequency OMP (JTF-OMP) method is proposed in this paper; the pilot subcarriers are divided into groups at the same interval and estimated separately. If the iteration corresponding to a group is terminated early due to the IN, meaning that this part of channels' estimation is not accuracy, then the estimation is adaptively weighted by the estimation of adjacent channels in time or frequency.

In addition, Doppler scale is also difficult to be estimated due to the IN, which is key to the subsequent OMP algorithm. Based on the guard interval insertion way, OFDM schemes can be categorized into three types: cyclic-prefix (CP), zero-padding (ZP), and time domain synchronization (TDS) OFDM [22–24]. In this paper, a CP-based adaptive Doppler scale estimation (ADSE) method is proposed; two shorter CPs for each OFDM symbol are generated and placed before two adjacent OFDM symbols, and a bank of parallel and self-correlator matched branches as [25] is used. Doppler scale estimation is performed by searching the branch with the largest self-correlator value, and two CPs can ensure the effective search in the IN cases. The main contributions can be summarized as follows:

(i) The proposed JTF-OMP method makes full use of the transient and intermittent feature of the IN occurring in time and frequency. The pilot subcarriers are grouped at the same interval and estimated separately; hence, some groups are not affected by the IN which is frequency selective, while the estimation of the affected channels can benefit adaptively from that of adjacent channels in time or frequency

(ii) The proposed ADSE method takes advantage of the randomness and transience of the IN occurring in time. On the premise of maintaining the same spectral and energy efficiency as traditional single CP structure, two shorter CPs with reasonable distance can ensure the self-correlation of the received signal in the IN cases, which is key to the Doppler scale estimation

(iii) The proposed algorithms do not require null subcarriers for channel estimation; hence, channel resource is saved. In addition, the proposed JTF-OMP method and ADSE method can be used in combination, alone, or embedded into other existing algorithms; they have good compatibility

The rest of this paper is structured as follows. The system model is discussed in Section 2, and the proposed ADSE method is presented in Section 3. Then, the JTF-OMP algorithm is deduced and realized in Section 4. The numerical results and analysis are illustrated in Section 5. Finally, the conclusion is drawn in Section 6.

Notation. The following notations will be used throughout this paper: Bold lowercase letters and uppercase letters denote the vectors and matrices, respectively. A^T, A^H, and A^{-1} denote the transpose, conjugate transpose, and inverse of A, respectively.

2. System Model

In this paper, a novel OFDM transmission structure is proposed matching to the ADSE method. As shown in Figure 1, it involves generating two identical CPs for each OFDM symbol, placed before two adjacent OFDM symbols. To maintain the same spectral and energy efficiency as traditional single CP structure, the CP length is set to half of the traditional.

Let T denote the OFDM symbol duration and T_{cp} the length of CP. Let K denote the number of subcarriers, and define $B = K/T$ the system bandwidth. The kth subcarrier is at frequency

Figure 1: The proposed novel OFDM transmission structure.

$$f_k = f_0 + \frac{k}{T}, k \in C, \tag{1}$$

where f_0 is the carrier center frequency and $C = \{-K/2, \cdots, K/2 - 1\}$ is the subcarrier set.

Let $x[k]$ denote the symbol transmitted on the kth subcarrier. The transmitted signal in baseband can be given as

$$s(t) = \sum_{k \in C} x[k] e^{j2\pi(k/T)t} g(t), \tag{2}$$

where $g(t)$ denotes the segmented rectangular windows of total length $T + 2T_{cp}$ as

$$g(t) = \begin{cases} 1, & t \in T_{int} \\ 0, & \text{otherwise} \end{cases}, \tag{3}$$

where $T_{int} = [-3T_{cp} - T, -2T_{cp} - T] \cup [-2T_{cp}, -T_{cp}] \cup [0, T]$.

Then, the corresponding passband signal can be written as

$$\tilde{s}(t) = \mathrm{Re}\left\{ e^{j2\pi f_0 t} \sum_{k \in C} x[k] e^{j2\pi(k/T)t} g(t) \right\} = \mathrm{Re}\left\{ \sum_{k \in C} x[k] e^{j2\pi f_k t} g(t) \right\}. \tag{4}$$

The channel impulse response for the time-varying UWA channel is often defined as

$$h(t, \tau) = \sum_l A_l(t) \delta(\tau - \tau_l(t)), \tag{5}$$

where $A_l(t)$ and $\tau_l(t)$ are the gain and time-varying delay of the lth path, respectively.

As in [25], the UWA OFDM symbol duration is around 100 ms to 200 ms, while the channel coherence time is usually on the order of seconds. Hence, for the duration $2T + 3T_{cp}$ shown in formula (3), the path gain can be assumed constant $A_l(t) \approx A_l$, and the time-varying delay can be reasonably approximated by a Doppler rate as

$$\tau_l(t) = \tau_l - a_l t, \tag{6}$$

where τ_l and a_l are the initial delay and Doppler scale of the lth path, respectively.

Hence, the channel model in (5) can be simplified to

$$h(t, \tau) = \sum_l A_l \delta(\tau - (\tau_l - a_l t)). \tag{7}$$

When the passband signal in (4) passes through the UWA channel described in (7), the received passband signal is

$$\begin{aligned} \tilde{r}(t) &= \tilde{s}(t) \otimes h(t, \tau) + \tilde{w}(t) \\ &= \mathrm{Re}\left\{ \sum_{k \in C} \sum_l x[k] A_l e^{j2\pi f_k((1+a_l)t - \tau_l)} \tilde{g}(t) \right\} + \tilde{w}(t), \end{aligned} \tag{8}$$

where $\tilde{g}(t) = g((1 + a_l)t - \tau_l)$ and $\tilde{w}(t) = \tilde{n}(t) + \tilde{v}(t)$ is the composite noise at passband.

By converting the passband signal $\tilde{r}(t)$ to baseband $r(t)$, satisfying $\tilde{r}(t) = \mathrm{Re}\{e^{j2\pi f_0 t} \cdot r(t)\}$, the following can be given

$$r(t) = \sum_{k \in C} \sum_l x[k] e^{j2\pi(k/T)((1+a_l)t - \tau_l)} \times A_l e^{j2\pi f_0(a_l t - \tau_l)} \tilde{g}(t) + w(t), \tag{9}$$

where $w(t) = n(t) + v(t)$, $n(t)$, and $v(t)$ are the composite noise, background noise, and IN at baseband, respectively.

3. Adaptive Preliminary Doppler Scale Estimation

According to literature [26], all the paths have approximately the same Doppler scale, i.e., $a_l \approx a$, and the small difference can be treated as additive noise. Then, the received baseband signal in (9) can be simplified as

$$r(t) = \sum_{k \in C} \sum_l x[k] e^{j2\pi(k/T)((1+a)t - \tau_l)} \cdot A_l e^{j2\pi f_0(at - \tau_l)} + w(t), \tag{10}$$

for $((1 + a)t - \tau_{max}) \in T_{int}$ corresponding to the rectangular window $\tilde{g}(t)$, where $\tau_{max} = \max_l \tau_l$.

Because two identical CPs are generated for each OFDM symbol as shown in Figure 1, some of the transmitted signal has a repetition pattern as

$$s(t) = s\left(t + T + T_{cp}\right), t \in T_{fro}, \tag{11}$$

where $T_{fro} = [-3T_{cp} - T, -2T_{cp} - T] \cup [-2T_{cp}, -T_{cp}]$.

As can be verified from (10), when the IN can be ignored, i.e., $w(t) = n(t)$, the received baseband signal still retains such a repetition pattern even after the UWA multipath propagation as

$$r(t) = e^{-j2\pi f_0(a/(1+a))\left(T + T_{cp}\right)} r\left(t + \frac{T + T_{cp}}{1 + a}\right), \tag{12}$$

for $((1 + a)t - \tau_{max}) \in T_{fro}$.

In fact, the IN cannot be completely removed at the receiver. But it has the randomness and transience feature occurring in time. As in formula (12), the received baseband signal retains the repetition pattern in two different time periods, because two identical CPs are designed in this

paper, i.e., T_{fro} includes $[-3T_{\text{cp}}-T,-2T_{\text{cp}}-T]$ and $[-2T_{\text{cp}}, -T_{\text{cp}}]$; the distance is $T+T_{\text{cp}}$. There is a great possibility that one of the time intervals is not affected by the IN. The problem is then to detect the repetition period to find the Doppler scale.

An ADSE method is proposed in this paper to find the Doppler scale based on the correlation metrics from the bank of self-correlators as shown in [25]. Assuming the oversampling time is $t_s = 1/\lambda B$, where the oversampling factor λ is an integer, then the oversampled baseband signal is $r[n] = r(t)|_{t=nt_s}$. The self-correlation metric can be given as

$$M\left(\tilde{K}, d\right) = \frac{\sum_{n=d}^{n=d+K'-1} r[n]r^*\left[n+\hat{K}\right]}{\sqrt{\sum_{n=d}^{n=d+K'-1}|r[n]|^2 \cdot \sum_{n=d}^{n=d+K'-1}|r^*[n+K\wedge]|^2}}, \tag{13}$$

where $\tilde{K}$, d, and K' are the window size, delay, and CP size, respectively.

As can be seen from (12), Doppler scale changes the period $T+T_{\text{cp}}$ to $(T+T_{\text{cp}})/(1+a)$; the optimal estimated window size $\hat{K}$ shall be $\lambda K(T+T_{\text{cp}})/T(1+\hat{a})$, where $\hat{a}$ is the estimated Doppler scale; hence, it can be estimated as

$$\hat{a} = \frac{\lambda K\left(T+T_{\text{cp}}\right) - T\hat{K}}{T\hat{K}}. \tag{14}$$

The CP size K' can be obtained by $\tilde{K}$ satisfying $K' = [\tilde{K}T_{\text{cp}}/(T+T_{\text{cp}})]$, where $[\cdot]$ means the integer rounding. The delay d is used to find the starting position of the two CPs.

The proposed ADSE algorithm is shown in Algorithm 1.

When the correlation metric of any branch exceeds the threshold in step 8, it means that a repetition pattern is detected. However, the repetition pattern occurs in two cases as shown in Figure 2. In case A, the correlation metric shown by marks 1 and 2 in Figure 2 is calculated at step 10. In case B, the correlation metric shown by marks 3 and 4 is calculated at step 11. Note that the positions d_s and $d_s - K_s$ may be negative, which are determined by the reference position. By obtaining the maximum value in step 12, the influence of the IN can be greatly weakened because it rarely appears in all the positions shown in Figure 2 at the same time, and the Doppler Scale can be estimated more accurately.

4. Joint Time-Frequency OMP Channel Estimation Algorithm

4.1. The Processing of the Received Signal. After the preliminary Doppler scale estimation, the received bandpass signal in (8) needs to be resampled according to the estimated Doppler Scale $\hat{a}$ to mitigate the Doppler effect, leading to

$$\tilde{z}(t) = \tilde{r}\left(\frac{t}{1+\hat{a}}\right) = \text{Re}\left\{\sum_{k\in\text{C}}\sum_{l} x[k]A_l e^{j2\pi f_k(((1+a_l)/(1+a\wedge))t-\tau_l)} g'(t)\right\} + w'(t), \tag{15}$$

where $g'(t) = g(((1+a_l)/(1+\hat{a}))t-\tau_l)$ and $w'(t)$ is the composite noise.

By converting the resampled passband signal $\tilde{z}(t)$ to the baseband $z(t)$, such that $\tilde{z}(t) = \text{Re}\{e^{j2\pi f_0 t}\cdot z(t)\}$, the following can be obtained

$$z(t) = \sum_{k\in\text{C}} x[k]\sum_{l} A_l e^{-j2\pi f_k\tau_l}\cdot e^{j2\pi f_0 c_l t}\cdot e^{j2\pi(k/T)(1+c_l)t} g'(t) + \bar{w}(t), \tag{16}$$

where $c_l = (a_l-\hat{a})/(1+\hat{a})$ is the residual Doppler scale and $\bar{w}(t) = \bar{n}(t) + \bar{v}(t)$, $\bar{n}(t)$, and $\bar{v}(t)$ are the composite noise, background noise, and IN at baseband, respectively.

Performing CP-OFDM demodulation, the output Y_m on the mth subchannel can be calculated as

$$Y_m = \frac{1}{T}\int_0^T z(t)e^{-j2\pi(m/T)t}dt = \sum_{k\in\text{C}} H[m,k]x[k] + \bar{w}_m, \tag{17}$$

where $H[m,k]$ is the transfer coefficient and $\bar{w}_m$ is the composite noise on the mth subchannel.

Collecting the $H[m,k]$ into the transfer matrix H, and the Y_m, $x[k]$, and $\bar{w}_m$ into vectors y, x, and w, respectively. Then, formula (17) can be denoted as

$$y = Hx + w. \tag{18}$$

Due to the delay spread and Doppler scale of the UWA channel, OFDM subcarriers lose their orthogonality, where coefficient $H[m,k]$ denotes the contribution of the kth subcarrier to the mth FFT output. According to (16) and (17), the following equation is satisfied

$$H[m,k] = \sum_{l} A_l e^{-j2\pi f_k\tau_l} \times \frac{1}{T}\int_0^T e^{j2\pi f_0 c_l t}\cdot e^{j2\pi(k/T)(1+c_l)t}\cdot e^{-j2\pi(m/T)t}dt, \tag{19}$$

where the value of the rectangular windows $g'(t)$ is one in the integral expression.

Set $\xi_{k,\tau} = e^{-j2\pi f_k\tau_l}$ and $f_{m,k,c} = (k-m+c_l(k+f_0T))/T$, leading to

$$\begin{aligned} H[m,k] &= \sum_{l} A_l\xi_{k,\tau}\cdot\frac{1}{T}\int_0^T e^{j2\pi f_{m,k,c}t}dt \\ &= \sum_{l} A_l\xi_{k,\tau}\cdot\frac{1}{j\pi f_{m,k,c}T}\int_0^T e^{j\pi f_{m,k,c}t}d\left(e^{j\pi f_{m,k,c}t}\right) \\ &= \sum_{l} A_l\xi_{k,\tau}\cdot e^{j\pi f_{m,k,c}T}\cdot\frac{\sin\left(\pi f_{m,k,c}T\right)}{\pi f_{m,k,c}T} = \sum_{l} A_l\xi_{k,\tau}\cdot\rho_{m,k,c}, \end{aligned} \tag{20}$$

where $\rho_{m,k,c} = \sin c(\pi f_{m,k,c}T)e^{j\pi f_{m,k,c}T}$.

Defining the mixing matrix $\boldsymbol{\Phi}(c)$ with (m,k)th element $[\boldsymbol{\Phi}(c)]_{m,k} = \rho_{m,k,c}$, and the diagonal matrix $\boldsymbol{\Lambda}(\tau)$ with kth element $[\boldsymbol{\Lambda}(\tau)]_{k,k} = \xi_{k,\tau}$, then the transfer matrix H can be expressed as

1: Initialize the self-correlation threshold M_{th}, maximum Doppler Scale $A_{\max}$
2: and initial delay d_0
3: Set $M_{\max} = 0$, $\widehat{K} = 0$, $\widehat{a} = 0$
4: Set $W_{\min} = [\lambda K(T + T_{cp})/T(1 + A_{\max})]$, $W_{\max} = [\lambda K(T + T_{cp})/T(1 - A_{\max})]$
5: **for** $d_s = d_0$ **to** $d_0 + W_{\max}$
6: **for** $K_s = W_{\min}$ **to** $W_{\max}$
7: Use (13) to calculate $M(K_s, d_s)$
8: **if** $|M(K_s, d_s)| > M_{th}$
9: $M_1 = |M(K_s, d_s)|$
10: $M_2 = |M(K_s, d_s + K_s)|$; $M_3 = |M(2K_s, d_s)|$
11: $M_4 = |M(K_s, d_s - K_s)|$; $M_5 = |M(2K_s, d_s - K_s)|$
12: $M_0 = \max_i(M_i)$
13: **if** $M_{\max} < M_0$ $M_{\max} = M_0$; $\widehat{K} = K_s$; **end if**
14: **end if**
15: **end for**
16: **end for**
17: **if** $\widehat{K} > 0$ Use (14) to calculate $\widehat{a}$; return $\widehat{a}$
18: **else** Go to step 1;
19: **end if**

Algorithm 1: The proposed ADSE algorithm.

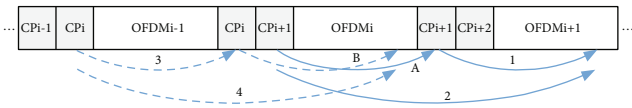

Figure 2: The possible location of the maximum correlation metric.

$$H = \sum_l A_l \mathbf{\Phi}(c) \mathbf{\Lambda}(\tau). \tag{21}$$

4.2. Sparse Channel Estimation. According to the sparsity of the UWA channel, applying compressed sensing theory to channel estimation can reduce the complexity of the algorithm. As in [27], an overcomplete dictionary of the delay and Doppler scale parameters is established in this paper, which can be expressed as

$$\tau_p \in \left\{ \frac{T}{\eta K}, \frac{2T}{\eta K}, \cdots, \tau_{\max} \right\}, \tag{22}$$

$$c_q \in \{-c_{\max}, -c_{\max} + \Delta c, \cdots, c_{\max}\}, \tag{23}$$

where the delay-resolution index η is an integer; $T/\eta K$ and Δc are the resolutions of the delay and Doppler scale, respectively; and $c_{\max}$ is the maximum value of c_l. A number of delay steps and Doppler steps are $N_\tau = \eta K \tau_{\max}/T$ and $N_c = 2c_{\max}/\Delta c + 1$, respectively. Hence, the gain of the lth path with delay τ_l and Doppler scale c_l can be denoted as $A_{p,q}$; the matrix H can be rewritten as

$$H = \sum_{p=1}^{N_\tau} \sum_{q=1}^{N_c} A_{p,q} \mathbf{\Phi}(c_q) \mathbf{\Lambda}(\tau_p). \tag{24}$$

Note that the channel model in (24) is not a BEM itself. However, considering that the UWA signal is a narrowband signal, the model reduces to the complex exponential BEM as shown in [27].

Then, formula (24) can be expressed equivalently as the following linear model

$$y = Fh + w, \tag{25}$$

$$F = \left[\mathbf{\Phi}(c_1) \mathbf{\Lambda}(\tau_1) x \quad \mathbf{\Phi}(c_2) \mathbf{\Lambda}(\tau_1) x \cdots \mathbf{\Phi}(c_{N_c}) \mathbf{\Lambda}(\tau_{N_\tau}) x \right], \tag{26}$$

$$h = \left[A_{1,1} \cdots A_{1,N_c} A_{2,1} \cdots A_{2,N_c} \cdots A_{N_\tau,N_c} \right]^T, \tag{27}$$

where F is the original sample set composed of the delay and residual Doppler scale and h is the set of the corresponding channel gains.

The UWA channels are naturally sparse, namely, most channel energy is concentrated in a few delay and/or Doppler values. Hence, h in (27) is sparse, and only some elements are not zero, which can be estimated by substituting the known pilot signal for y in (25). In this paper, OMP-based algorithm is considered, which is the most representative one among the CS algorithms. Since the composite noise w in (25) includes the IN which appears transient and intermittent in time and frequency, part of the channels' estimation will be affected.

To resolve this problem, the pilot subcarriers are divided into groups at the same interval and estimated separately. Let N_P denote the number of pilot subcarriers, and N_G denotes the number of groups on the premise that $N_E = N_P/N_G$ is an integer. Then, formulas (25) and (26) can be rewritten as

$$y_{P_i} = F_{P_i} h + w_{P_i}, \tag{28}$$

$$F_{P_i} = \left[S_i \mathbf{\Phi}(c_1) \mathbf{\Lambda}(\tau_1) x_{P_i} \cdots S_i \mathbf{\Phi}(c_{N_c}) \mathbf{\Lambda}(\tau_{N_\tau}) x_{P_i} \right], \tag{29}$$

1: Initialize the resolution related parameters η and Δc,
2: the maximum values $\tau_{\max}$ and $c_{\max}$;
3: Input the received signal y, transmitted pilots x_P, previous estimation h_0,
4: the number of groups N_G and decision indexes σ, $\varepsilon(\varepsilon < 0.01)$;
5: Initialize the vectors $h = 0$, $\beta = 1$, and coefficient $\gamma(\gamma < 0.5)$;
6: for$i$ = 1toN_G
7: Extract y_{P_i} and x_{P_i} from y and x_P, respectively; Set S_i;
8: Use (29) to calculate F_{P_i}; Set $z = y_{P_i}$, $A = F_{P_i}$;
9: Initialize the iteration number $j = 1$, residual vector $r_0 = z$,
10: the atomic index set $b_0 = \emptyset$ and estimated channel vector $\widehat{\hbar}_0 = 0$;
11: **while** $\|r_j\|^2 \geq \varepsilon\|z\|^2$ or $\|\hbar\wedge_j\|^2 \geq \sigma$
12: Find the optimal index $\lambda_j = \arg \max_{n=1,2,\cdots,N_\tau N_c} |\langle a_n, r_{k-1}\rangle|$;
13: Update the index set $b_j = [b_{j-1}, \lambda_j]$;
14: Set $X_j = A_{b_j}$, consisting of columns of A indexed by b_j;
15: Compute $\widehat{\hbar}_j = (X_j{}^H X_j)^{-1} X_j{}^H r_{j-1}$;
16: Update the residual vector $r_j = r_{j-1} - X_j\widehat{\hbar}_j$; $j = j + 1$;
17: **end while**
18: $h_i = \widehat{\hbar}_{j-1}$
19: if $\|h_i\|^2 < \sigma$ $\beta_i = \gamma$; **end** if
20: **end** for
21: $h = \sum_i \beta_i h_i / \sum_i \beta_i$;
22: if $\sum_i \beta_i < N_G/2$ $h = (h_0 + \gamma h)/(1 + \gamma)$; **end** if
23: return h;

Algorithm 2: The proposed JTF-OMP algorithm.

where y_{P_i}, F_{P_i}, w_{P_i}, and x_{P_i} are the received signal, part of the transfer matrix, part of the noise, and transmitted pilots corresponding to the ith group pilots, respectively. S_i is the selection matrix that selects the elements in Y that correspond to nonzero entries in the ith group pilots.

The proposed OMP-based algorithm is shown in Algorithm 2. It is named JTF-OMP because the estimation of the affected channels can benefit adaptively from that of adjacent channels in time or frequency.

When $\|r_j\|^2 \geq \varepsilon\|z\|^2$ is not satisfied in step 11, it means that the residual vector is small enough and the channel estimation is accurate. When $\|\hbar\wedge_j\|^2 \geq \sigma$ is not satisfied, it indicates that the remaining estimated taps are resulted by the IN according to literature [17], where σ is decided by the power of transmitted signals, the power of the IN, and the number of pilots. Then, this part of channel estimation needs to be multiplied by a coefficient γ in step 19. The overall channel estimation h is obtained by the weighted addition of each h_i in step 21. Hence, the estimation of the affected channels benefits adaptively from that of adjacent channels in frequency. Finally, the judgement is done in step 22. If the partial estimation is interrupted many times due to the IN, meaning that the IN is serious, then the channel estimation is corrected adaptively by the value in the previous OFDM-period. In a word, the proposed JTF-OMP algorithm makes full use of the transient and intermittent feature of the IN occurring in time and frequency.

5. Simulation and Analysis

In this section, the performance of the proposed algorithms is presented and compared through Monte Carlo simulations, in terms of the normalized mean square error (NMSE) and the bit-error-rate (BER). The NMSE is defined as

$$\text{NMSE} = \frac{\sum_{i=1}^{N} |h_i - h_i|^2}{\sum_{i=1}^{N} |h_i|^2}, \tag{30}$$

where h_i and h_i denote the real and the estimated channel impulse response, respectively.

The simulation parameters are depicted as follows. The CP-OFDM specifications are consistent with [28] except for the CP structure. The carrier center frequency, bandwidth, number of subcarriers, number of pilots, symbol duration, subcarrier spacing, and CP length are summarized in Table 1. The pilot subcarriers are distributed on every fourth subcarrier. There are no null subcarriers; the remaining 768 subcarriers are used for data symbols. All of the symbols are encoded with a rate 1/2 nonbinary LDPC code and modulated by QPSK constellations.

The number of discrete paths is 15, and the delay difference between adjacent paths follows an exponential distribution with the average value ψ. To reflect different scenarios over distances, ψ is within the range of 0.2 ~ 1 ms. The amplitude follows a Rayleigh distribution with the average power decreasing exponentially with the delay. The Doppler

Table 1: Parameters of CP-OFDM in numerical simulation.

Parameter	Notation	Value
Center frequency	f_0	13 kHz
System bandwidth	B	9.77 kHz
No. subcarriers	K	1024
No. pilots	N_P	256
Symbol duration	T	104.86 ms
Subcarrier spacing	$\Delta f \coloneqq 1/T$	9.54 Hz
CP length	T_{cp}	12.3 ms

scale is Gaussian distributed with the mean 0 and standard deviation D. The resolution of the Doppler scale in the overcomplete dictionary is set to be 0.01 m/s.

The composite noise w in (25) is modeled as two-component Gaussian mixture (GM) model, which is widely used to study the IN environment [20]. The probability density function of the noise on the mth subchannel is modelled as

$$f(w[m]) = (1-\theta)\mathcal{N}\left(0, \sigma_n^2\right) + \theta\mathcal{N}\left(0, \sigma_n^2 + \sigma_v^2\right), \tag{31}$$

where $\mathcal{N}(\cdot)$ is the complex Gaussian distribution function and θ is the IN occurrence probability (INOP). σ_n^2 and σ_v^2 are the variances of the background noise and IN, respectively. In the following simulations, θ is within the range of $0 \sim 0.1$; accordingly, about $0 \sim 100$ IN samples are generated within one OFDM block. In addition, σ_n^2 and σ_v^2 are varied to generate different signal-to-noise ratio (SNR).

In Figure 3, the NMSE performance of the proposed algorithms versus SNR is evaluated under different T_{cp} and ψ. As can be seen, when the ψ is smaller, the smaller T_{cp} has little loss of performance. However, when the ψ gets larger enough, the smaller T_{cp} makes the performance worse obviously. The proposed ADSE method involves generating two shorter identical CPs for each OFDM symbol, as shown in Figure 1. In order to maintain the same spectral and energy efficiency as traditional single CP structure, the CP length is set to be 12.3 ms, i.e., half of the traditional value which is 24.6 ms. Herein, the length of the guard interval has not been changed. The difference is that only half of the OFDM tail data has been copied to the CP. Therefore, the proposed two CPs structure can also well mitigate the effect of the intersymbol interference (ISI) and intercarrier interference (ICI). Meanwhile, high estimation accuracy is maintained when the ψ is not large enough, corresponding to the small or medium distance UWA environment.

Figure 4 shows the BER performance versus INOP under different number of groups N_G, where σ_n^2 and σ_v^2 are kept at the values so that the SNR is 16 dB when the INOP is 0.02. When the INOP is larger, the BER performance is improved with the increase of N_G. However, when N_G increases further, the BER performance deteriorates gradually. It is because that appropriate grouping can make good use of

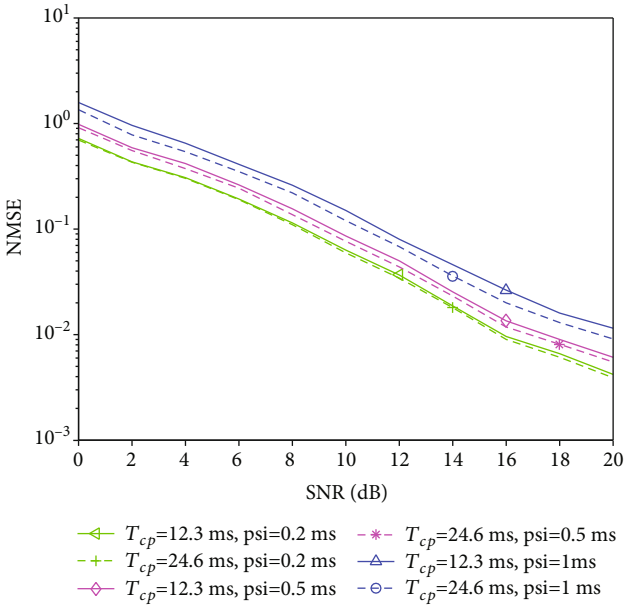

Figure 3: The NMSE performance versus SNR under different T_{cp} and ψ (for $N_G = 2$, $D = 0.2$ m/s, $\eta = 3$, $\lambda = 3$, and $\theta = 0.02$).

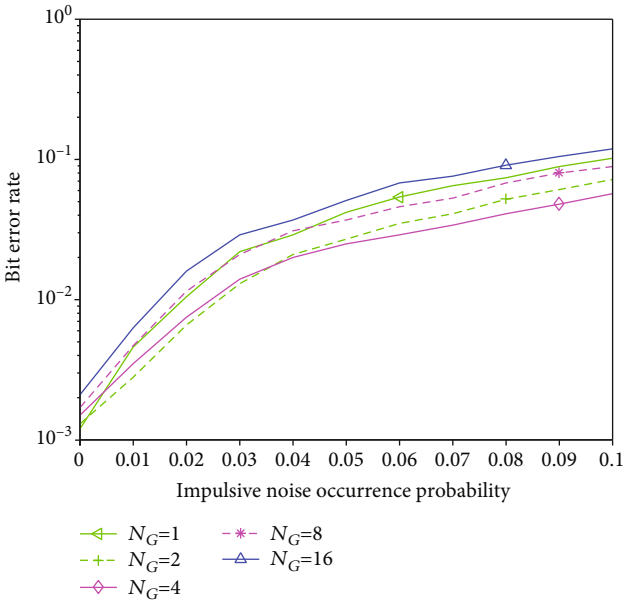

Figure 4: The BER performance versus INOP under number of groups N_G (for $D = 0.2$ m/s, $\psi = 0.5$ ms, $\eta = 3$, $\lambda = 3$, and $\theta = 0.02$).

the estimation of the channels which are not affected by the random IN. But, too many groups will lead to too few pilot subcarriers, which degrades the channel estimation. In fact, N_G needs to be adjusted adaptively according to the actual number of the pilot subcarriers. In the current simulation configuration, setting N_G to be 2 or 4 is a relatively good choice.

Figure 5 shows the BER performance versus SNR under different standard deviation D. The notation ADSE in the

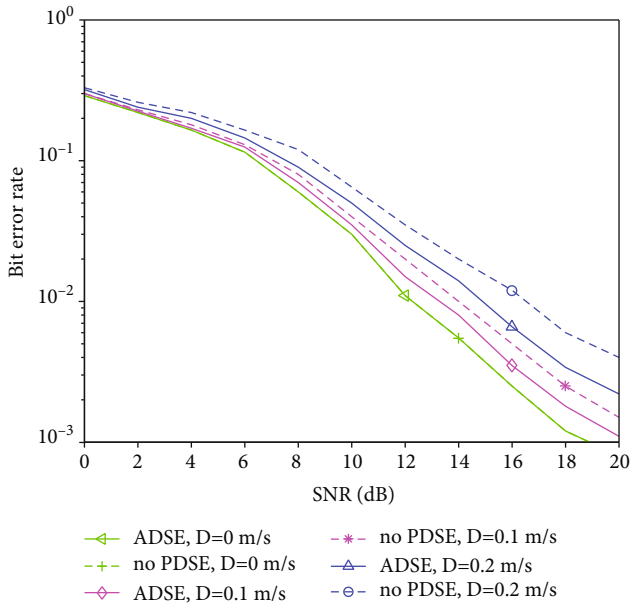

Figure 5: The BER performance versus SNR under different D (for $N_G = 2$, $\psi = 0.5$ ms, $\eta = 3$, $\lambda = 3$, and $\theta = 0.02$).

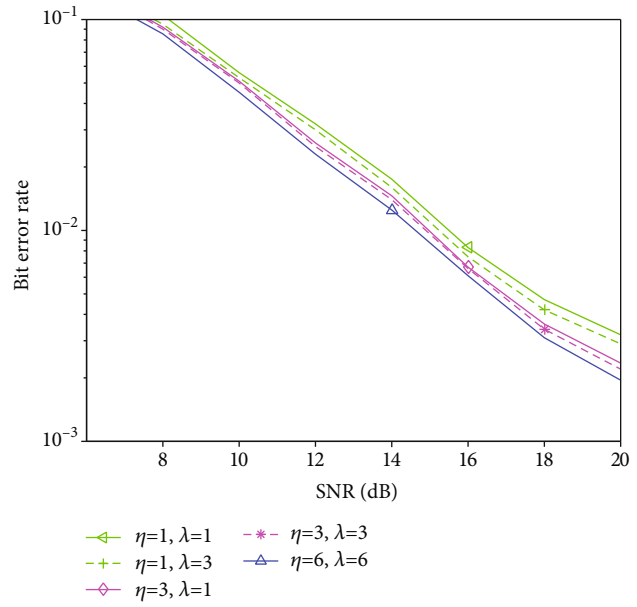

Figure 6: The BER performance versus SNR under different η and λ (for $N_G = 2$, $D = 0.2$ m/s, $\psi = 0.5$ ms, and $\theta = 0.02$).

figure means that the Doppler scale is estimated by the proposed ADSE algorithm. The notation no PDSE means that the Doppler scale is not preliminarily estimated, i.e., $\widehat{a} = 0$ in (15) and $c_l = a_l$ in (16). As can be seen, BER is decreased significantly through the ADSE algorithm when the SNR is higher, and the improvement is more obvious with the increase of Doppler scale. Because the Doppler effect is mitigated through the ADSE algorithm, i.e., c_l is much closer to 0 than a_l; accordingly, the overcomplete dictionary of Doppler scale in (23) gets much smaller. This shows that the ADSE algorithm can improve the accuracy and convergence speed of the JTF-OMP algorithm.

In Figure 6, the BER performance under different η and λ is evaluated. It can be observed that the performance is improved with the increase of η, but the improvement saturates quickly. It is because that the increase of the dictionary size of the delay can better reflect the discrete nature of the channel in continuous time. In addition, the oversampling factor $\lambda > 1$ increases the performance slightly. Clearly, the Doppler scale can be better estimated through finer self-correlation metric in (13). However, larger η and λ increase the computational complexity. To achieve better comprehensive performance, η and λ have both adaptively set to be 3 in the current simulation configuration.

In Figure 7, the NMSE performance of the proposed algorithms is compared with the A-OMP [17], the OMP [14], and the least-square (LS) algorithm, respectively. The notation DSE in the figure means that the Doppler scale is preliminarily estimated by the DSE algorithm [25]. As can be observed, the CS-based algorithms significantly outperform the LS-based algorithm. This can be explained by the fact that the former better exploit the sparsity of the UWA channels. Meanwhile, the proposed algorithms integrating JTF-OMP with ADSE can achieve NMSE performance

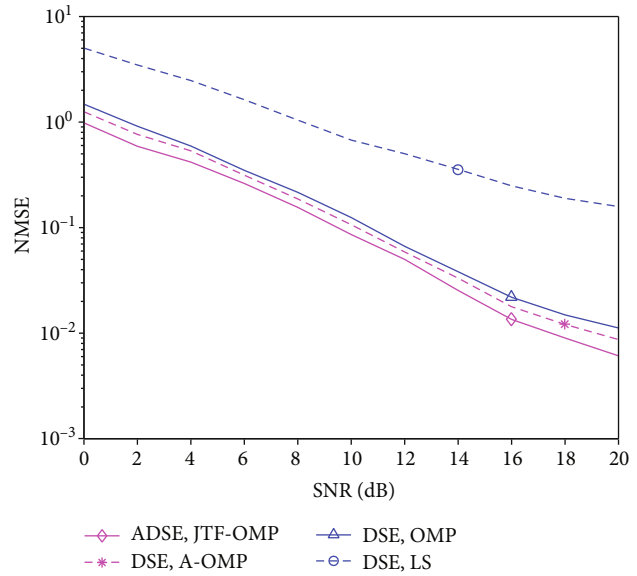

Figure 7: Comparison of the NMSE versus SNR among the proposed, the A-OMP, the OMP, and the LS (for $N_G = 2$, $D = 0.2$ m/s, $\psi = 0.5$ ms, $\eta = 3$, $\lambda = 3$, and $\theta = 0.02$).

advantages under all SNR cases, because the interference problem of the IN has been better considered and dealt with.

Figures 8 and 9 show the BER performance of these algorithms. As can be seen, the proposed algorithms always maintain the best BER performance, while the OMP algorithm with no PDSE has always been the worst. There are performance gaps between the JTF-OMP and the two others and gaps between the ADSE and the two others. The results also show that the JTF-OMP and the ADSE can be

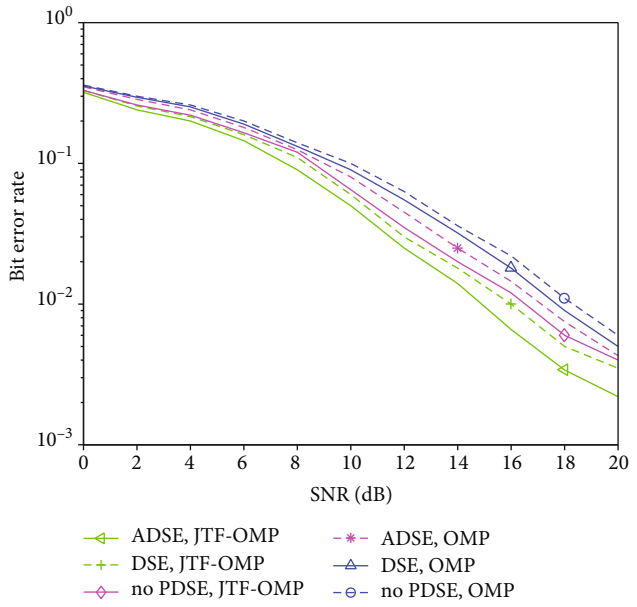

Figure 8: Comparison of the BER performance versus SNR between the proposed algorithms and the OMP (for $N_G = 2$, $D = 0.2$ m/s, $\psi = 0.5$ ms, $\eta = 3$, $\lambda = 3$, and $\theta = 0.02$).

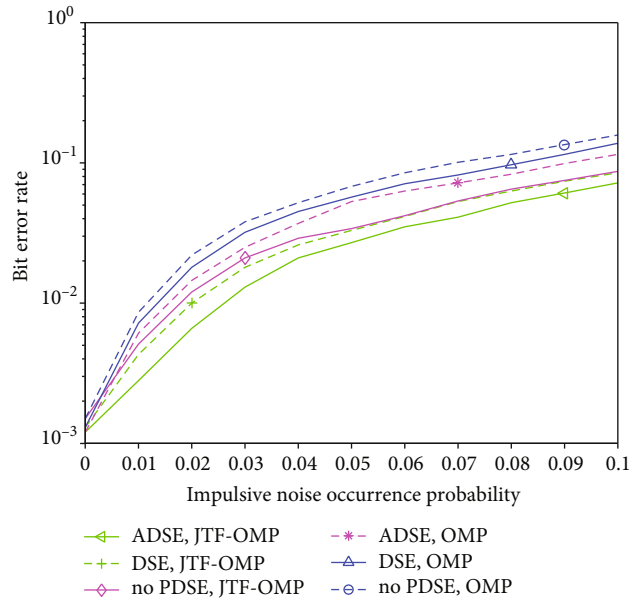

Figure 10: Comparison of the BER performance versus INOP between the proposed algorithms and the OMP (for $N_G = 2$, $D = 0.2$ m/s, $\psi = 0.5$ ms, $\eta = 3$, and $\lambda = 3$).

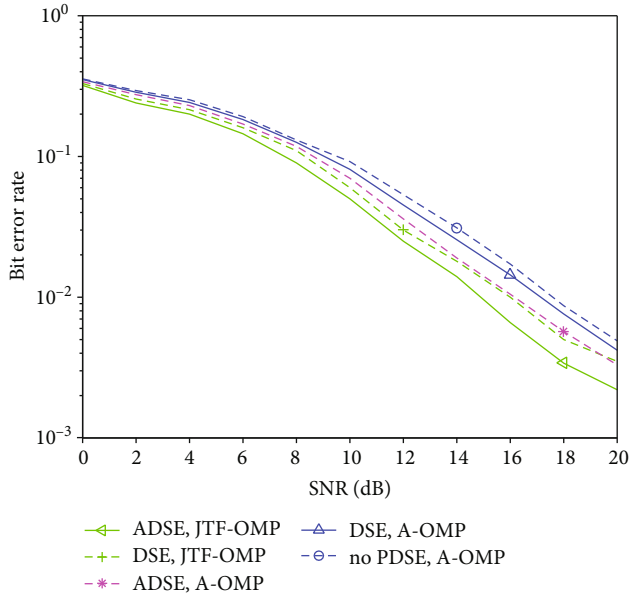

Figure 9: Comparison of the BER performance versus SNR between the proposed algorithms and the A-OMP (for $N_G = 2$, $D = 0.2$ m/s, $\psi = 0.5$ ms, $\eta = 3$, $\lambda = 3$, and $\theta = 0.02$).

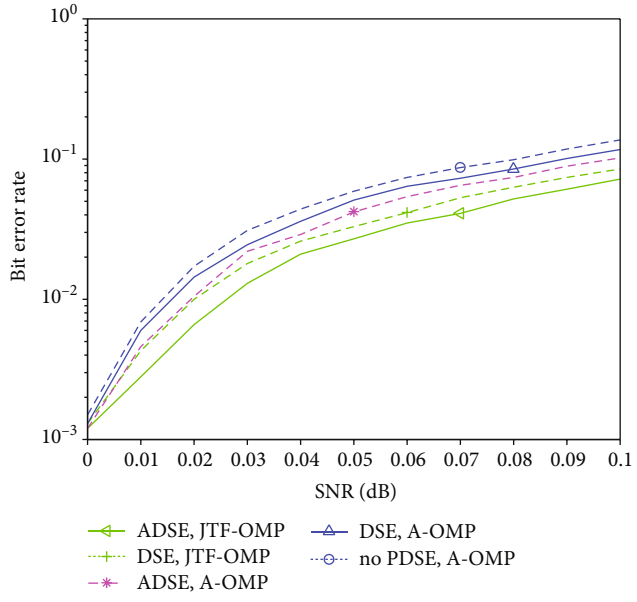

Figure 11: Comparison of the BER performance versus INOP between the proposed algorithms and the A-OMP (for $N_G = 2$, $D = 0.2$ m/s, $\psi = 0.5$ ms, $\eta = 3$, and $\lambda = 3$).

adaptively embedded into other existing algorithms, and some performance gain can be achieved.

In Figures 10 and 11, the BER performance of these algorithms versus INOP is evaluated, where the values of σ_n^2 and σ_ν^2 are consistent with Figure 4. It can be found that the proposed algorithms integrating JTF-OMP with ADSE remain the best BER performance with the increase of INOP. The performance gaps between these algorithms are similar to Figures 8 and 9. Obvious, the proposed algorithms can achieve much higher estimation accuracy and better system reliability than others in the IN environment. It can be explained that the JTF-OMP and the ADSE have made full use of the transient and intermittent feature of the IN occurring in time and frequency, and the impact of the IN has been greatly mitigated.

6. Conclusions

Considering the UWA communication in impulsive noise environment, adaptive algorithms integrating JTF-OMP with ADSE are proposed in this paper. In the ADSE method, on the premise of maintaining the same spectral and energy efficiency as traditional single CP structure, two shorter identical CPs for each OFDM symbol are generated and placed before two adjacent OFDM symbols. By searching the branch with the largest self-correlator value related to the two CPs, the Doppler scale can be estimated effectively in the IN cases. In the JTF-OMP algorithm, the pilot subcarriers are divided into groups at the same interval, and the estimation is adaptively weighted by the estimation of adjacent channels in time or frequency according to the severity of IN. The proposed algorithms do not require null subcarriers for channel estimation; hence, channel resource is saved. Simulation results verify the validity of the proposed algorithms; much higher estimation accuracy and better system reliability can be achieved in the IN environment. Our future research work will focus on the cross-layer channel estimation techniques via acknowledge/not-acknowledge (ACK/NAK) feedback for UWA communication in the IN environment.

Data Availability

The MATLAB Source Code data used to support the findings of this study are available from the corresponding author upon request.

Conflicts of Interest

The authors declare that they have no conflicts of interest.

Acknowledgments

This work was supported by the Zhejiang Provincial Natural Science Foundation of China under Grant LY18F010001, the Ningbo Natural Science Foundation of China under Grant 2019A610076, the Humanities and Social Science Research Project of the Ministry of Education of China under Grant 20YJAZH130, the Public Technology Research Project of Zhejiang under Grant LGF20F020004, and the Natural Science Foundation of China under Grant 61571250.

References

[1] G. L. Zhou, Y. M. Li, Y. C. He, and X. L. Wang, "Artificial fish swarm based power allocation algorithm for MIMO-OFDM relay underwater acoustic communication," *IET Communications*, vol. 12, no. 9, pp. 1079–1085, 2018.

[2] X. Zhuo, M. Liu, Y. Wei, G. Yu, F. Qu, and R. Sun, "AUV-aided energy efficient data collection in underwater acoustic sensor networks," *IEEE Internet of Things Journal*, vol. 7, no. 10, pp. 10010–10022, 2020.

[3] B. S. Sharif, J. Neasham, O. R. Hinton, and A. E. Adams, "A computationally efficient Doppler compensation system for underwater acoustic communications," *IEEE Journal of Oceanic Engineering*, vol. 25, no. 1, pp. 52–61, 2000.

[4] Y. Li, S. Wang, C. Jin, Y. Zhang, and T. Jiang, "A survey of underwater magnetic induction communications: fundamental issues, recent advances, and challenges," *IEEE Communications & Surveys Tutorials*, vol. 21, no. 3, pp. 2466–2487, 2019.

[5] Y. Li, X. H. Chen, S. L. Sun, Z. C. Tan, and X. Tao, "Virtual time-inverse OFDM underwater acoustic channel estimation algorithm based on compressed sensing," *Journal of Sensors*, vol. 2020, 12 pages, 2020.

[6] G. Leus and P. A. van Walree, "Multiband OFDM for covert acoustic communications," *IEEE Journal on Selected Areas in Communications*, vol. 26, no. 9, pp. 1662–1673, 2008.

[7] S. J. Hwang and P. Schniter, "Efficient multicarrier communication for highly spread underwater acoustic channels," *IEEE Journal on Selected Areas in Communications*, vol. 26, no. 9, pp. 1674–1683, 2008.

[8] W. Li and J. C. Preisig, "Estimation of rapidly time-varying sparse channels," *IEEE Journal of Oceanic Engineering*, vol. 32, no. 4, pp. 927–939, 2007.

[9] C. R. Berger, S. L. Zhou, J. C. Preisig, and P. Willett, "Sparse channel estimation for multicarrier underwater acoustic communication: from subspace methods to compressed sensing," *IEEE Transactions on Signal Processing*, vol. 58, no. 3, pp. 1708–1721, 2010.

[10] Y. Zhang, R. Venkatesan, O. A. Dobre, and C. Li, "Efficient estimation and prediction for sparse time-varying underwater acoustic channels," *IEEE Journal of Oceanic Engineering*, vol. 45, no. 3, pp. 1112–1125, 2020.

[11] F. Yu, D. Li, Q. Guo, Z. Wang, and W. Xiang, "Block-FFT based OMP for compressed channel estimation in underwater acoustic communications," *IEEE Communications Letters*, vol. 19, no. 11, pp. 1937–1940, 2015.

[12] Y. Zhou, F. Z. Zeng, and Y. C. Gu, "A gradient descent sparse adaptive matching pursuit algorithm based on compressive sensing," in *Proceedings of the IEEE International Conference on Machine Learning and Cybernetics*, pp. 464–469, Jeju, South Korea, February 2016.

[13] N. U. R. Junejo, H. Esmaiel, M. Z. Zhou, H. X. Sun, J. Qi, and J. F. Wang, "Sparse channel estimation of underwater TDS-OFDM system using look-ahead backtracking orthogonal matching pursuit," *IEEE Access*, vol. 6, pp. 74389–74399, 2018.

[14] E. Panayirci, M. T. Altabbaa, M. Uysal, and H. V. Poor, "Sparse channel estimation for OFDM-based underwater acoustic systems in Rician fading with a new OMP-MAP algorithm," *IEEE Transactions on Signal Processing*, vol. 67, no. 6, pp. 1550–1565, 2019.

[15] S. Anwar, C. Yuen, H. X. Sun, Y. L. Guan, and Z. Babar, "A novel receiver design of nonorthogonal FDM systems in underwater acoustics communication," *IEEE Systems Journal*, vol. 14, no. 3, pp. 3875–3884, 2020.

[16] E. Panayirci, M. T. Altabbaa, and H. V. Poor, "Channel estimation and equalization for Alamouti SF-coded OFDM-UWA communications," *IEEE Transactions on Vehicular Technology*, vol. 70, no. 2, pp. 1709–1723, 2021.

[17] Z. Z. Wang, Y. Z. Li, C. C. Wang, D. H. Ouyang, and Y. L. Huang, "A-OMP: an adaptive OMP algorithm for underwater acoustic OFDM channel estimation," *IEEE Wireless Communications Letters*, vol. 10, no. 8, pp. 1761–1765, 2021.

[18] M. Chitre, J. Potter, and S. Ong, "Optimal and near-optimal signal detection in snapping shrimp dominated ambient noise," *IEEE Journal of Oceanic Engineering*, vol. 31, no. 2, pp. 497–503, 2006.

[19] M. Nassar, P. Schniter, and B. L. Evans, "A factor graph approach to joint OFDM channel estimation and decoding in impulsive noise environments," *IEEE Transactions on Signal Processing*, vol. 62, no. 6, pp. 1576–1589, 2014.

[20] P. Chen, Y. Rong, S. Nordholm, and Z. He, "Joint channel and impulsive noise estimation in underwater acoustic OFDM systems," *IEEE Transactions on Vehicular Technology*, vol. 66, no. 11, pp. 10561–10571, 2017.

[21] X. R. Lv, Y. M. Li, Y. Q. Wu, and H. Liang, "Kalman filter based recursive estimation of slowly fading sparse channel in impulsive noise environment for OFDM systems," *IEEE Transactions on Vehicular Technology*, vol. 69, no. 3, pp. 2828–2835, 2020.

[22] H. Esmaiel and D. C. Jiang, "Zero-pseudorandom noise training OFDM," *Electronics Letters*, vol. 50, no. 9, pp. 650–652, 2014.

[23] X. Ma, F. Yang, S. C. Liu, W. B. Ding, and J. Song, "Structured compressive sensing-based channel estimation for time frequency training OFDM systems over doubly selective channel," *IEEE Wireless Communications Letters*, vol. 6, no. 2, pp. 266–269, 2017.

[24] H. Esmaiel and D. C. Jiang, "Spectrum and energy efficient OFDM multicarrier modulation for an underwater acoustic channel," *Wireless Personal Communications*, vol. 96, pp. 1577–1593, 2017.

[25] S. Mason, C. R. Berger, S. Zhou, and P. Willett, "Detection, synchronization, and Doppler scale estimation with multicarrier waveforms in underwater acoustic communication," *IEEE Journal on Selected Areas in Communications*, vol. 26, no. 9, pp. 1638–1649, 2008.

[26] B. Li, S. Zhou, M. Stojanovic, L. Freitag, and P. Willett, "Multicarrier communication over underwater acoustic channels with nonuniform Doppler shifts," *IEEE Journal of Oceanic Engineering*, vol. 33, no. 2, pp. 198–209, 2008.

[27] C. R. Berger, Z. Wang, J. Z. Huang, and S. Zhou, "Application of compressive sensing to sparse channel estimation," *IEEE Communications Magazine*, vol. 48, no. 11, pp. 1–11, 2010.

[28] P. Qarabaqi and M. Stojanovic, "Statistical characterization and computationally efficient modeling of a class of underwater acoustic communication channels," *IEEE Journal of Oceanic Engineering*, vol. 38, no. 4, pp. 701–717, 2013.